

Investigation of mean wind pressures on 'E' plan shaped tall building

Biswarup Bhattacharyya^a and Sujit Kumar Dalui*

Department of Civil Engineering, Indian Institute of Engineering Science and Technology, Shibpur, Howrah – 711103, India

(Received September 14, 2017, Revised January 12, 2018, Accepted January 27, 2018)

Abstract. Due to shortage of land and architectural aesthetics, sometimes the buildings are constructed as unconventional in plan. The wind force acts differently according to the plan shape of the building. So, it is of utter importance to study wind force or, more specifically wind pressure on an unconventional plan shaped tall building. To address this issue, this paper demonstrates a comprehensive study on mean pressure coefficient of 'E' plan shaped tall building. This study has been carried out experimentally and numerically by wind tunnel test and computational fluid dynamics (CFD) simulation respectively. Mean wind pressures on all the faces of the building are predicted using wind tunnel test and CFD simulation varying wind incidence angles from 0° to 180° at an interval of 30°. The accuracy of the numerically predicted results are measured by comparing results predicted by CFD with experimental results and it seems to have a good agreement with wind tunnel results. Besides wind pressures, wind flow patterns are also obtained by CFD for all the wind incidence angles. These flow patterns predict the behavior of pressure variation on the different faces of the building. For better comparison of the results, pressure contours on all the faces are also predicted by both the methods. Finally, polynomial expressions as the *sine* and *cosine* function of wind angle are proposed for obtaining mean wind pressure coefficient on all the faces using Fourier series expansion. The accuracy of the fitted expansions are measured by sum square error, R^2 value and root mean square error.

Keywords: wind tunnel test; computational fluid dynamics; irregular plan shaped building; mean pressure coefficients; Fourier series expansion

1. Introduction

Advancement of light-weight materials and construction technology have made ease to build up high-rise buildings. These buildings are mostly susceptible to earthquake and wind loading. Generally, these loads are devastating in nature. Out of these two types of loading, investigation of wind effects on high-rise building is the focal point of the present study. Moreover, it is of utter importance to study wind effects on tall buildings. The pressure variation of some common plan shaped buildings (e.g., square, rectangular, circular) are available in the reference codes (AS/NZS 1170-2 2011; ASCE 7-10 2010; BS 6399-2 1997; IS 875 (Part 3) 2015). But, pressure variation on different faces of peculiar plan shaped tall buildings are also peculiar.

One of the design parameter to consider wind load in the structural design is mean pressure coefficient. In general, buildings are designed considering mean pressure coefficient for a particular face and mean pressure coefficient may vary highly in case of unconventional plan shaped tall buildings. Thus, it is important to investigate mean wind pressures on different faces of an unconventional plan shaped tall building. Also, pressure contour on different faces of a building may provide an idea of pressure variation. It has been reported in several researches (Bandi *et al.* 2013, Dalui 2008, Tanaka *et al.*

2012) that with the change of plan shape of a building, the impact of pressure variation is very higher. To address this issue, wind effects on full scale building (Bashor *et al.* 2012, Li *et al.* 1998, 2007) is considered to be most reliable method in computing wind pressure. However, this is not feasible in the real scenario many times. In this aspect, wind tunnel test (Endo *et al.* 2006, Gomes *et al.* 2005, Kim and Kanda 2013, Li *et al.* 2013, 2006, Tanaka *et al.* 2012, Wang *et al.* 2013, Yi and Li 2015) is widely accepted method to quantify wind pressure on different faces of a building. Several studies have been carried out by the researchers using wind tunnel test to assess wind effects on building in past two decades. Kim and You (2002) investigated dynamic response of tapered tall building under wind excitation. The experiment was carried out with four building models of different tapered ratio in urban flow condition using wind tunnel. It was found that along wind response was insignificant as compared to the across wind response for the tapered buildings. Gu and Quan (2004) tested 15 different models of typical tall building in wind tunnel to investigate across-wind dynamic force obtained from first mode. Gomes *et al.* (2005) carried out experimental study by wind tunnel test on 'L' and 'U' plan shaped building. Kim *et al.* (2008) investigated tapering effect on the *rms* across-wind displacement response of tall building by wind tunnel test. This study was conducted using aerolastic model and tapering effect was noticed with high reduced velocity and moderate structural damping ratio of 2-4%. Whereas, Amin and Ahuja (2012) predicted wind effects on two rectangular shaped interfering buildings placed in the close proximity such that it acted as an 'L' and 'T' plan shaped building. In both the cases, experimental

*Corresponding author, Assistant Professor

E-mail: sujit_dalui@rediffmail.com

^a Former Post Graduate student

E-mail: biswarupb6@gmail.com

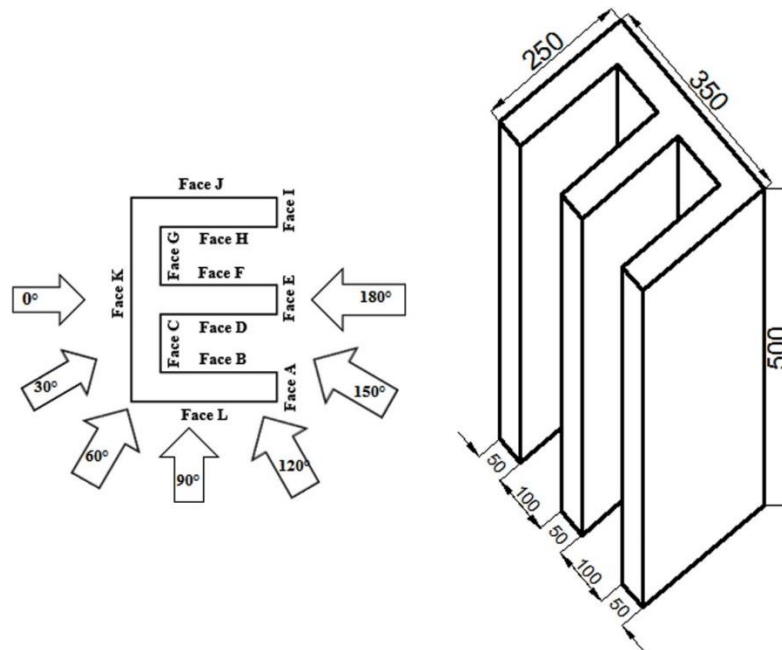


Fig. 1 Different faces and isometric view of the building model

study was carried out by wind tunnel test. Bandi *et al.* (2013) investigated aerodynamic characteristics of different triangular plan shaped tall buildings with aerodynamic modifications using wind tunnel test. Yi and Li (2015) made a full-scale as well as wind tunnel study on a super tall building situated in Hong Kong. To measure force and pressure coefficient, high frequency force balance and synchronize multi-pressure sensors are used respectively in wind tunnel. The responses taken from wind tunnel was seen to be quite comparable with the full-scale results. In order to compute wind effects on 'L' plan shaped tall building under dynamic across wind, wind tunnel test was also conducted by Li and Li (2016). They proposed empirical formula to quantify across-wind dynamic load on 'L' plan shaped tall building considering side ratio and terrain category as the variable. Such empirical formula can help a practicing engineer to quantify wind load directly without rigorous formulation. The accuracy in predicting wind effects on buildings by wind tunnel test has already established well through all the above-mentioned studies. However, efficiency of experimental study is still questionable.

With the enhancement of computational facility, numerical methods for the prediction of wind effects on building has emerged a lot. In this regards, Computational Fluid Dynamics (CFD) (Chakraborty *et al.* 2014, Cheung and Liu 2011, Gomes *et al.* 2003, Hargreaves and Wright 2007, Huang *et al.* 2011, 2007, Swaddiwudhipong and Khan 2002, Zhang *et al.* 2005) is the tool to quantify wind effects efficiently as well as more accurately. Several studies have already established the applicability of CFD under wind excitation. Some of these researches are briefly discussed here. Swaddiwudhipong and Khan (Swaddiwudhipong and Khan 2002) investigated wind induced dynamic response of tall building using CFD.

Mainly $k-\epsilon$ and LES turbulence model were used for numerical simulation and further the results were compared with wind tunnel results. Numerically predicted vortex shedding phenomenon was comparable with experiment for uniform flow using $k-\epsilon$ model but, it failed to predict the shedding frequency for fluctuating incoming flow. Furthermore, a comparative study between two mostly used turbulence models i.e., LES and $k-\epsilon$ Reynolds-average Navier-Stokes (RANS) model have been conducted by Cheng *et al.* (2003). Numerical study was conducted over a matrix of cubes using these two turbulence models. Both the models predicted well the mean flow condition within the array of cubes but, LES outperforms $k-\epsilon$ model in predicting the span wise mean velocity and Reynolds stress. These two models were also adopted in computation of wind effects on the Commonwealth Advisory Aeronautical Council (CAARC) building (Huang *et al.* 2007). LES predicted better result for mean and dynamic wind loading on the building, while $k-\epsilon$ model yields promising results more efficiently. Chakraborty *et al.* (2014) carried out a comparative study between experimental and numerical method to predict wind effect on '+' plan shaped tall building. Similar study has also been conducted in (Mukherjee *et al.* 2014) to investigate wind pressure on 'Y' plan shaped tall building. In both the cases, results predicted by numerical technique were within the acceptable limit with respect to the wind tunnel results. All the above-mentioned studies are suggesting the applicability of experimental and numerical technique in terms of accuracy and efficiency for the prediction of wind effects on different buildings. However, very limited research work is presented on unconventional plan shaped tall buildings.

In the present study, wind effects on 'E' plan shaped tall building is studied experimentally as well as numerically. More specifically, mean wind pressures on different faces of

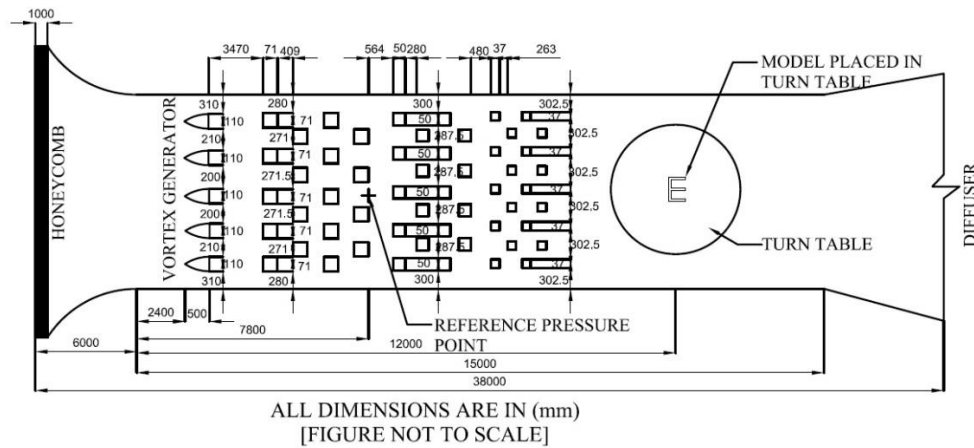


Fig. 2 Model placed in wind tunnel (plan view)

the 'E' plan shaped tall building are studied for different wind incidence angle varies from 0° to 180° at an equal interval of 30° (Fig. 1). Experimental study is carried out using wind tunnel test and numerical study is performed using RANS $k-\varepsilon$ model by CFD. Mean pressure coefficient (C_p) on the different faces of the building is proposed experimentally as well as numerically as the main goal of this study. The results found from numerical study are compared with wind tunnel test data in order to check applicability of CFD technique for this building. Along with this, wind flow pattern around the building for all the wind incidence angles are studied using CFD. Also, pressure contours on different faces of the 'E' plan shaped building are studied using both the methods. Finally, polynomial expressions for the prediction of mean pressure coefficients on each of the faces are proposed using Fourier series expansion as the *sine* and *cosine* function of wind incidence angle. The accuracy of the proposed models are checked by several procedures.

2. Experimental study

2.1 Experimental setup

The experiment has been carried out in an open circuit boundary layer wind tunnel (Fig. 2) at Wind Engineering Centre, Department of Civil Engineering, Indian Institute of Technology Roorkee, India. The cross section of the wind tunnel was 2 m (width) \times 2 m (height) with a length of 38 m. A square section of 6 m \times 6 m holed honeycomb with the thickness of 1 m is located at the entrance of the wind tunnel to generate uniform wind flow throughout the wind tunnel. An elliptical effuse profile of length 6 m with contraction ratio of 9.5:1 is situated just after the honeycomb at the inlet region for smoothening the wind flow inside the tunnel. Boundary layer wind flow was created by placing vortex generator (width 110 mm) at the inlet region. Square cubes of three different dimensions (7.1 cm, 5.0 cm, 3.7 cm) were installed in three different layers at the inlet region to carry out the experiment under terrain

category II as per IS 875 (Part 3): 2015 (IS 875 (Part 3) 2015). A turn table is located at 12 m from the elliptical effuse. Pressure measurement model was fitted at the center of turn table. Pressure on the different faces of building model was measured by rotating the turn table for different wind angles. The wind tunnel has uniform section (i.e., 2 m \times 2 m) upto 15 m from the elliptical effuse and rest of the portion is diffuser. Wind speed can be varied between 2 m/s and 10 m/s by controlling dynodrive attached with the fan located at the end of diffuser portion. A pitot tube is located at 7.8 m from the elliptical effuse to measure wind speed inside wind tunnel and also reference pressure point is located at the same region. To measure pressure, one end of the pressure tapping was connected to pressure transducer and another end was connected with reference pressure point. These pressure values were recorded in 'Barron' instrument and saved in computer through 'Datataker'. The data was saved in a computer which was connected with the transducer.

2.2 Details of model

The model was made of Perspex sheet having thickness of 4 mm at a scale of 1:300 (Fig. 3). Different faces and isometric view of the model with detail dimensions are shown in Fig. 1. A total 210 numbers of pressure tapping points (Fig. 4) were installed at five different height of 10 mm, 100 mm, 250 mm, 400 mm and 490 mm from bottom on all the faces of the model. The pressure tapings were made of steel tubes with 1 mm internal diameter and 15-20 mm long. These pressure tapings were installed in the model by drilling holes at each and every grid point and very close to the edges of the faces to study the changes of pressure variations due to separations, upwash and downwash mechanisms of flow.

2.3 Boundary condition

Wind tunnel test has been conducted at wind speed of 10 m/s. Boundary layer flow was generated by vortex generator and cubic blocks placed in the upstream side of



Fig. 3 Model placed inside wind tunnel

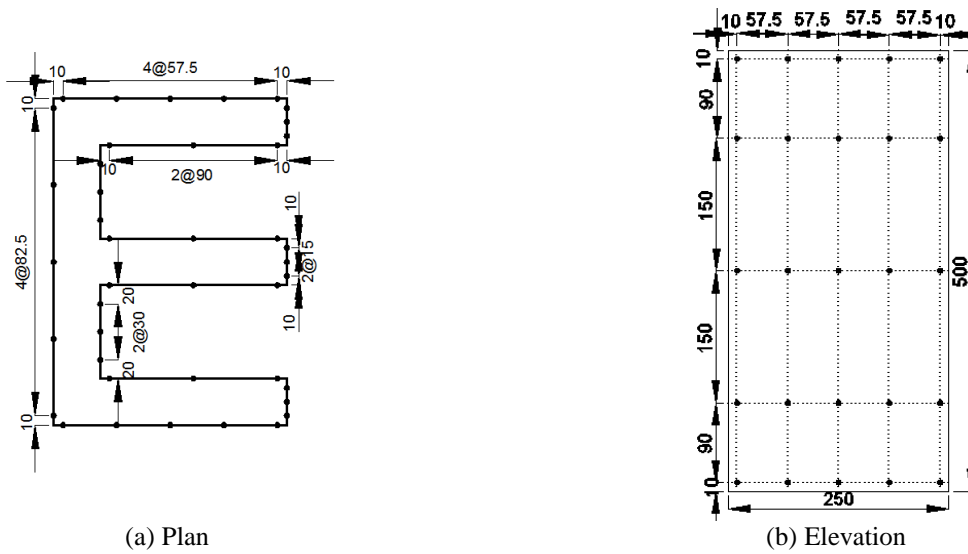


Fig. 4 Pressure tapings installed in the model

the wind tunnel. The power law index (α) for the velocity profile inside the wind tunnel is 0.133. The model was placed at the center of the turn table located at 12 m from elliptical effuse. Free stream velocity was measured using pitot tube during the experiment. The measured boundary layer wind flow profile and turbulence intensity profile are plotted in Fig. 7.

3. Numerical study

Numerical study has been carried out by Computational Fluid Dynamics (CFD). Standard RANS $k-\varepsilon$ turbulence model is used for the modelling because it maintains a trade-off between computational efficiency and accuracy. The standard $k-\varepsilon$ model uses the gradient diffusion hypothesis to relate the Reynold stresses to the mean velocity gradients and turbulent viscosity. k is turbulence kinetic energy and is defined as the variance of fluctuations in velocity and ε is the turbulence eddy dissipation (the rate at which the velocity fluctuation dissipate).

So, modified continuity and momentum equation after incorporating two new variables i.e., k and ε are

$$\frac{\partial \rho}{\partial t} + \frac{\partial}{\partial x_j} (\rho U_j) = 0 \quad (1)$$

$$\frac{\partial \rho U_i}{\partial t} + \frac{\partial}{\partial x_j} (\rho U_i U_j) = -\frac{\partial p'}{\partial x_i} + \frac{\partial}{\partial x_j} \left[\mu_{eff} \left(\frac{\partial U_i}{\partial x_j} + \frac{\partial U_j}{\partial x_i} \right) \right] + S_M \quad (2)$$

where S_M is the sum of body forces, μ_{eff} is the effective viscosity accounting for turbulence and p' is the modified pressure. The $k-\varepsilon$ model, like the zero equation model, is based on the eddy viscosity concept, so that

$$\mu_{eff} = \mu + \mu_t \quad (3)$$

where μ_t is the turbulence viscosity. The $k-\varepsilon$ model assumes that the turbulence viscosity is linked to the turbulence kinetic energy and dissipation via the relation

$$\mu_t = C_\mu \rho \frac{k^2}{\varepsilon} \quad (4)$$

where C_μ is a constant.

The value of k and ε can be obtained directly from the differential transport equations for the turbulence kinetic energy and turbulence dissipation rate

$$\frac{\partial(\rho k)}{\partial t} + \frac{\partial}{\partial x_j}(\rho U_j k) = \frac{\partial}{\partial x_j} \left[\left(\mu + \frac{\mu_t}{\sigma_k} \right) \frac{\partial k}{\partial x_j} \right] + P_k - \rho \varepsilon + P_{kb} \quad (5)$$

$$\frac{\partial(\rho \varepsilon)}{\partial t} + \frac{\partial}{\partial x_j}(\rho U_j \varepsilon) = \frac{\partial}{\partial x_j} \left[\left(\mu + \frac{\mu_t}{\sigma_\varepsilon} \right) \frac{\partial \varepsilon}{\partial x_j} \right] + \frac{\varepsilon}{k} (C_{\varepsilon 1} P_k - C_{\varepsilon 2} \rho \varepsilon + C_{\varepsilon 1} P_{\varepsilon b}) \quad (6)$$

P_k is turbulence production due to viscous forces, which is modeled using

$$P_k = \mu_t \left(\frac{\partial U_i}{\partial x_j} + \frac{\partial U_j}{\partial x_i} \right) \frac{\partial U_i}{\partial x_j} - \frac{2}{3} \frac{\partial U_k}{\partial x_k} \left(3\mu_t \frac{\partial U_k}{\partial x_k} + \rho k \right) \quad (7)$$

C_μ is the k - ε turbulence model constant of value 0.09. $C_{\varepsilon 1}$, $C_{\varepsilon 2}$ are also k - ε turbulence model constant in CFD of values 1.44, 1.92 respectively. σ_k is the turbulence model constant for k equation of value 1.0 and σ_ε is the turbulence model constant for ε equation of value 1.3. ρ is the density of air in the model and taken as 1.224 kg/m^3 . μ and μ_t are dynamic and turbulent viscosity respectively. The other notations are having their usual meanings. The building was considered as bluff body in CFD and the flow pattern around the building is studied using this model. Turbulence intensity is considered as 10%.

3.1 Domain and meshing

The domain size (Fig. 5) is taken as referred in Franke *et al.* (2004). The upstream side is considered as $5H$ from the face of the building, downstream side is taken as $15H$ from the face of the building, two side clearance of the domain is taken as $5H$ from the face of the building and top clearance is also taken as $5H$ from the top surface of the building. Such large size of domain helps in vortex generation at the leeward side of the building and backflow of wind can also be prevented. Finite volume discretization approach is used to discretize the whole domain so that, separation of wind flow, upwash and downwash mechanisms can be happened similar to the experimental study. Finite element mesh is generated using tetrahedral elements throughout the domain (Fig. 6). Tetrahedron meshing is inflated near the model with hexagonal elements for uniform wind flow near the surface of the 'E' plan shaped tall building. Around 1 million elements are generated in total within the whole domain.

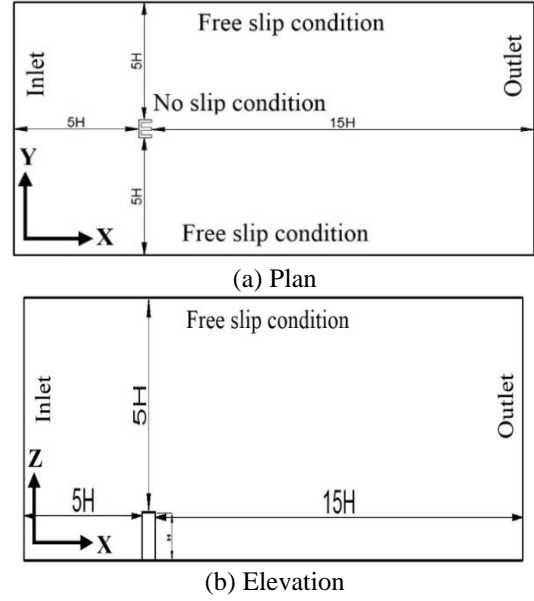


Fig. 5 Domain for the numerical study

3.2 Boundary condition

The boundary conditions are taken as the same as used in the wind tunnel test such that the results found from the numerical analysis can be compared with the experimentally predicted results. Similar types of boundary condition were also used in Chakraborty *et al.* (2014). Boundary layer wind flow from the inlet side is generated using the Power law as given in Eq. (8) and the coefficient (α) is taken as 0.133 which was found from the experiment.

$$\frac{U}{U_0} = \left(\frac{z}{z_0} \right)^\alpha \quad (8)$$

where U_0 is the basic wind speed and is taken as 10 m/s and z_0 is the boundary layer height which is considered as 1 m similar to the wind tunnel test. The velocity profile and turbulence intensity profile in the inlet for experimental and numerical study are shown in Fig. 7 and it is seen that numerically predicted wind flow is comparable with the experimental study. Turbulence intensity is also comparable, but some discrepancy is noticeable. However, this discrepancy can be minimized with improving the mesh pattern or, by increasing the number of elements in the domain. This figure is suggesting that the numerical model is acceptable for computing wind effects on the building. Relative pressure at outlet is considered as 0 Pa. The velocity in all other directions is set to zero. Residual target for convergence is set as 1×10^{-5} . Side surfaces and top surface of the domain are taken as free slip condition so that no shear stress generates over these surfaces and all surfaces of the building and ground of the domain are considered as no slip condition to measure the pressure contour accurately.

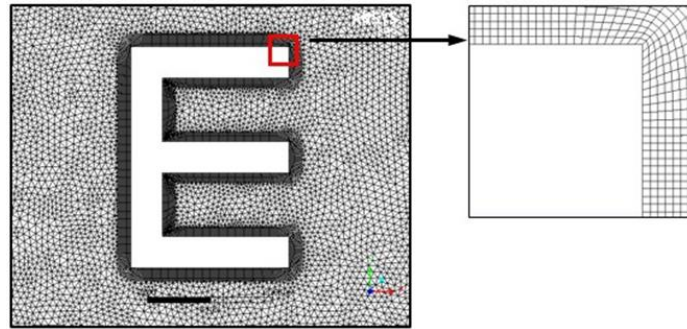


Fig. 6 Mesh pattern around the building (plan view)

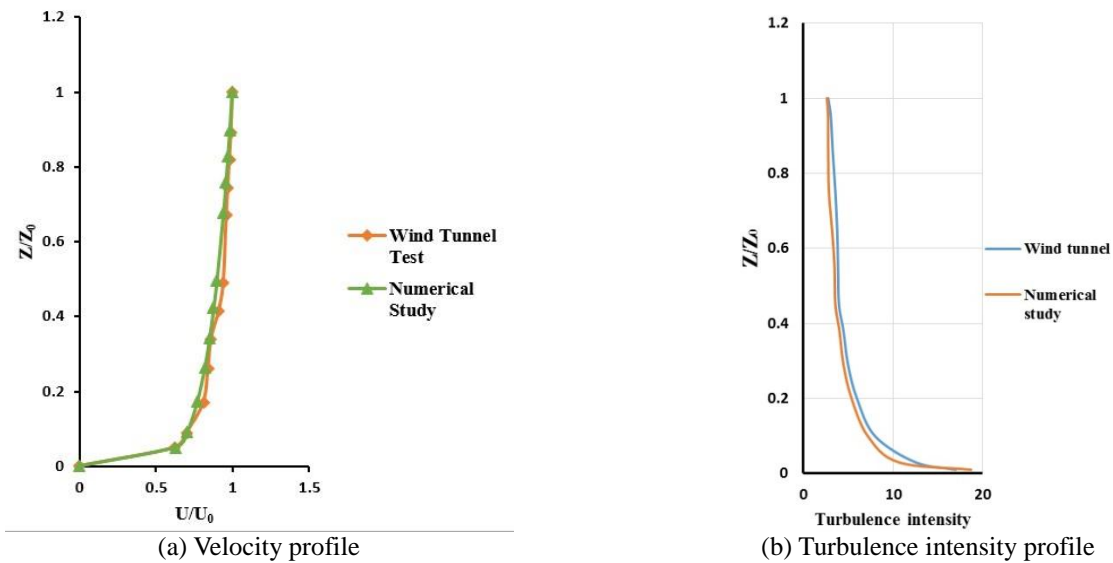


Fig. 7 Comparison of experimentally and numerically predicted wind speed and turbulence intensity

4. Results and discussion

4.1 Wind flow pattern

Pressure variation on the building is directly influenced by wind flow pattern. Vortex generation and different types of mechanism such as separation of flow, upwash and downwash are happened due to dynamic behavior of wind flow. To investigate such mechanisms more accurately, wind flow patterns around the 'E' plan shaped tall building are being studied for different wind incidence angles varying from 0° to 180° at an interval of 30° using CFD technique. Flow pattern for different wind incidence angles are shown in Fig. 8.

It is clearly seen that flow pattern around the model is symmetrical about vertical axis for 0° and 180° wind incidence angle, so it is expected to get similar pressure distribution on symmetrical faces for these two wind angles. Face K and E may be experienced symmetrical pressure distribution about vertical axis for 0° and 180° wind angle because of perpendicular wind direction about these two faces. Also, wind flow pattern is almost symmetrical for 90° wind angle, however flow lines are not symmetrical after separation, because sectional view of two sides are

unsymmetrical and vortices generated on these two sides are not symmetrical. Vortex generation and variation of pressure are fully dependent on the plan shape of the building. Dynamic nature of wind flow is observed for other wind incidence angles due to assymetry in the cross sectional area in plan. Negative pressure may observe in the rear side faces with respect to wind flow directions in each case due to suction force of vortices at the wake region. Also negative pressure will occur at the flow separation zone. Some small vortices generated in between the limbs of 'E' plan shaped tall building due to interference effects of the limbs and negative pressure may occur on these surfaces also.

4.2 Variation of pressure coefficients

It is of utter importance to study pressure coefficients in a detail way for every unconventional plan shaped tall building which can be used by designer to design the building under wind excitation. Critical pressure coefficients may not be found in perpendicular wind incidence angles only (Chakraborty *et al.* 2014, Mukherjee *et al.* 2014). For that reason, a detail investigation of wind pressure variation is required to carry out with skew wind

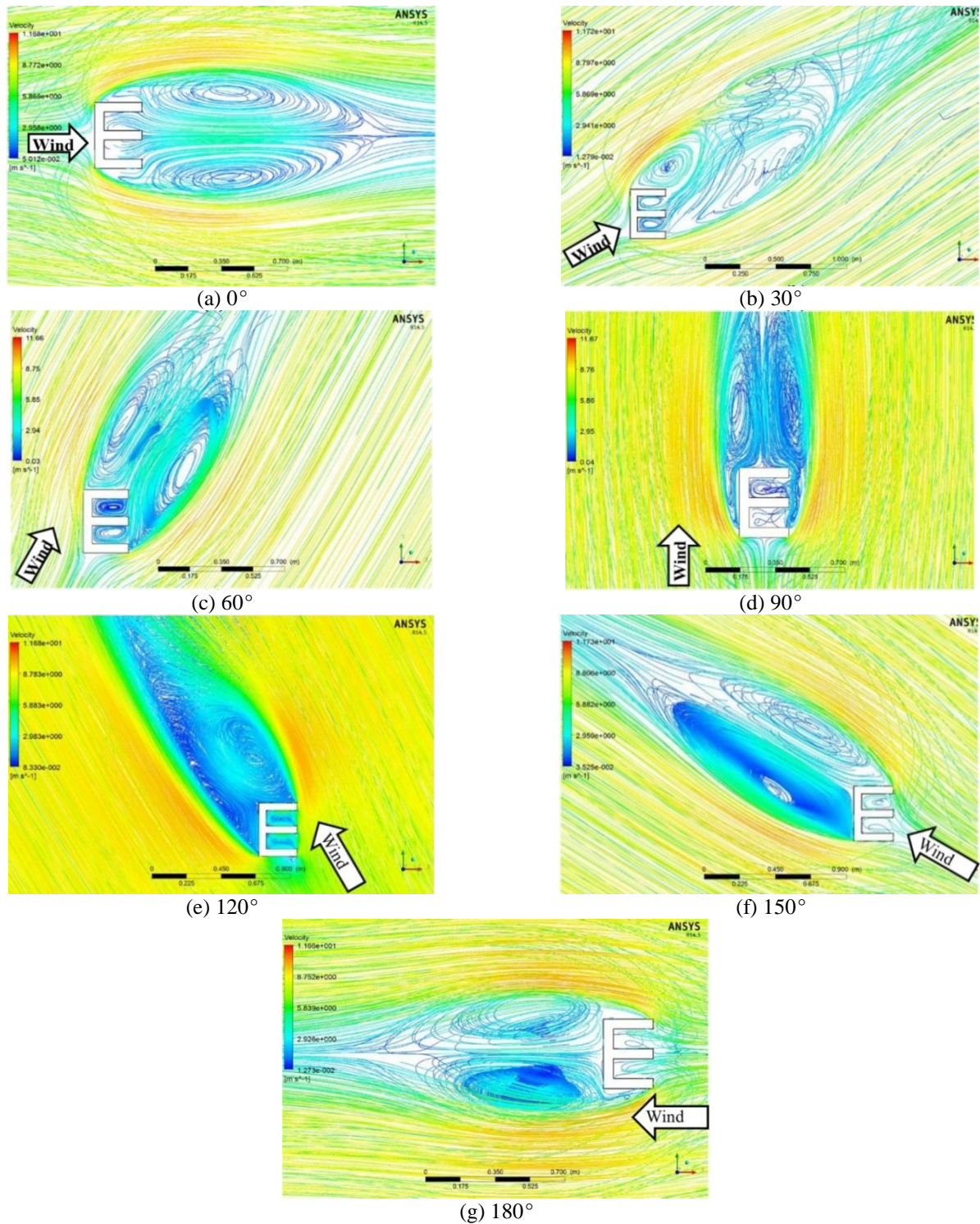


Fig. 8 Wind flow pattern for different wind incidence angles

angles also. In this aspect, a detail investigation of pressure coefficient and pressure variation on different faces of 'E' plan shaped tall building has been carried out experimentally as well as numerically by wind tunnel test and CFD technique respectively. Wind pressure variation is measured for 0° to 180° wind incidence angle at an equal interval of 30°.

4.2.1 Experimental results

Pressure contour on different faces are plotted for every wind incidence angle. Some critical pressure contours are shown in Fig. 9 for all the faces. Also, mean pressure coefficients of all the faces are shown in Fig. 11(a). Generally buildings are designed considering mean pressure coefficients, but it is desired to design any building face considering local pressure coefficients of any point on that face.

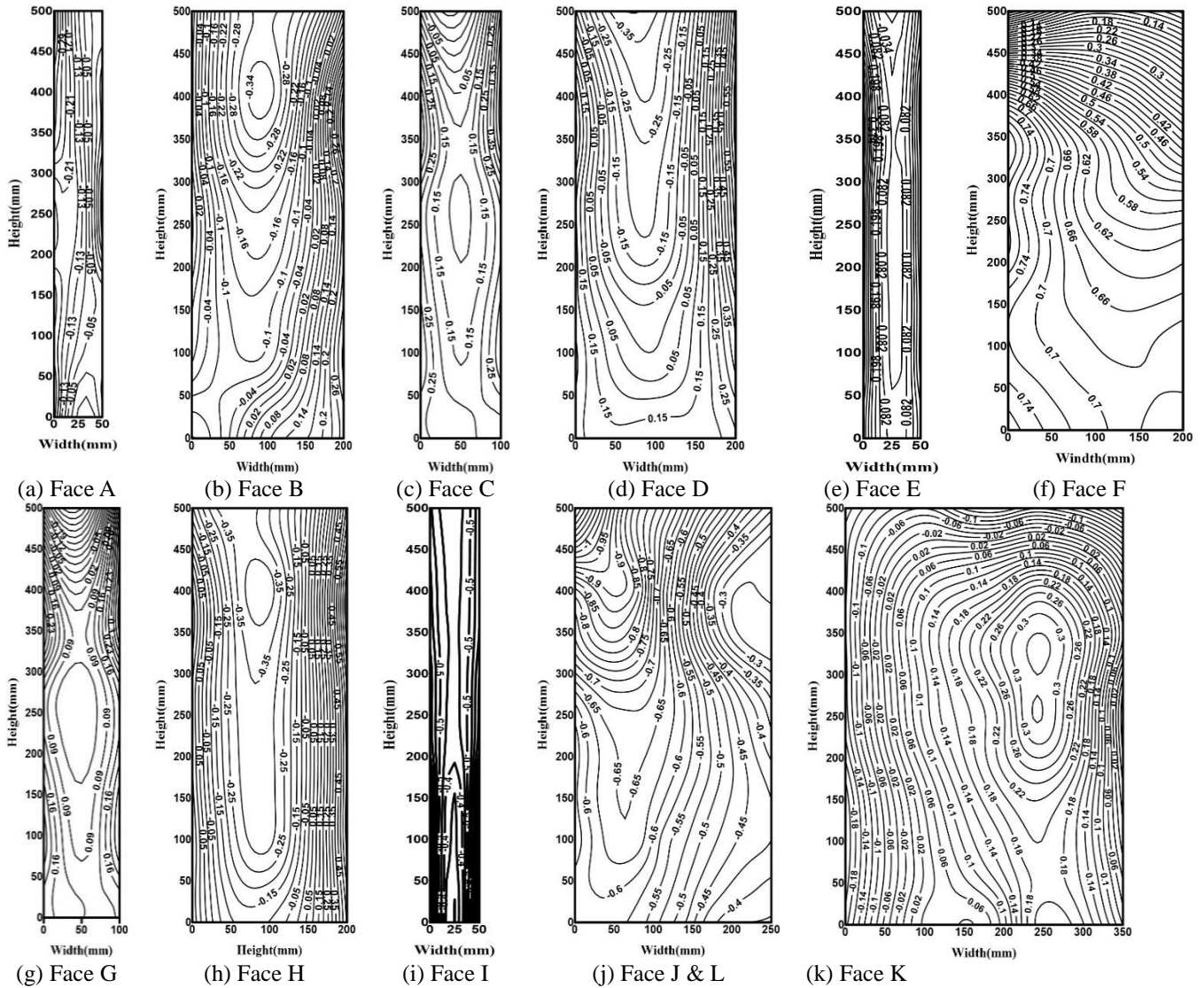


Fig. 9 Pressure contour on different faces of the model (Wind tunnel results) at different wind angles; (a) 120°, (b) 120°, (c) 120°, (d) 120°, (e) 120°, (f) 180°, (g) 120°, (h) 120°, (i) 60°, (j) 180° and (k) 60°

Wind is directly affecting face K and E for wind incidence angle 0° and 180° respectively, so the pressure distribution is symmetrical about vertical axis and vortices generated at the wake region is also symmetrical for both the cases (Fig. 8). Pressure distribution on the rear side faces are also symmetrical for these two wind incidence angles due to the similar reason. Face J always undergoes negative pressure as no direct wind forces is acting on that surface. Higher variation of mean pressure coefficient is noticed on face A (-0.68 to 0.62) with the variation of wind incidence angle from 0° to 180°. Whereas, least significant variation of pressure coefficient is noticed on face F, G, H, I. For different wind incidence angles, these four faces are least affected. However from the symmetrical point of view, these faces are also similar important as face D, C, B, A.

Maximum critical mean pressure coefficients (C_p) on face A, B, C, D are noticed at 90° wind incidence angle. On the other hand, critical mean C_p on face E, F, G, H, J, L are found at 180° wind incidence angle. Maximum mean C_p on

face I and face K are found for wind incidence angle 60° and 0° respectively. It is also noticeable that some of the faces are experienced almost zero mean C_p (Fig. 11(a)) at some wind incidence angles. In spite of almost zero mean pressure coefficients on face B, E, G, H, K, L (Fig. 11(a)) for wind incidence angle 120°, 60° and 30°, these faces are more critical under design consideration as the variation of pressure is perceptible. Almost same pressure variation of intensities from negative to positive is noticed on these faces which creates thrust as well as suction type of force on a face. This nature of wind force is very critical from design point of view.

It is noticeable that more critical faces are B, E, G, H, K, L under design consideration due to larger deviation of pressure contour on these faces. Maximum positive mean C_p on face E and K are occurred at 180° and 0° wind incidence angle respectively. However, maximum positive mean C_p on face (A, I), (B, H), (C, G), (D, F) and (J, L) are occurred at 150°, 180°, 180°, 180° and 120° wind angles

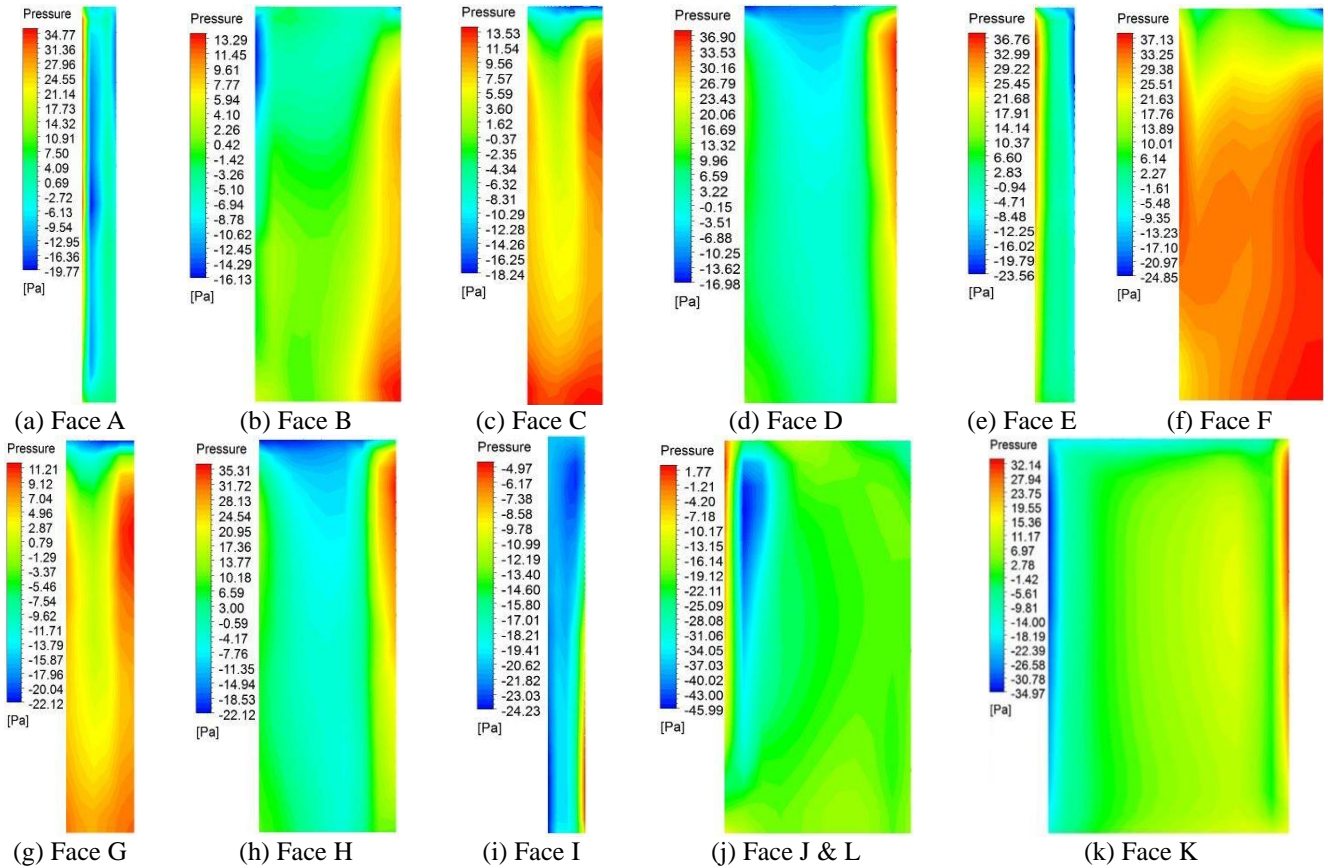


Fig. 10 Pressure contour on different faces of the model (CFD results) at different wind angles; (a) 120°, (b) 120°, (c) 120°, (d) 120°, (e) 120°, (f) 180°, (g) 120°, (h) 120°, (i) 60°, (j) 180° and (k) 60°

respectively. Although, maximum mean C_p on face (J, L) occurred at 120° wind angle, it is noticed that mean C_p at 90° wind angle is almost same with 120° wind angle. On the other hand, maximum negative mean C_p on face (A, I), (B, H), (C, G), (D, F), (J, L), K and E are occurred at 90°, 90°, 90°, 90°, 180°, 90° and 90° wind angle respectively. It is perceptible that, maximum negative mean C_p on all the faces are occurred at perpendicular wind incidence angles. However, for the case of maximum positive mean C_p , skew wind angles are also made impact for some of the faces. Critical face considering maximum positive mean pressure coefficient (0.8) is face K under wind inclination angle 180° and critical face considering maximum negative mean pressure coefficient (-0.68) is face A under wind inclination angle 90°.

4.2.2 Numerical results

Detail pressure variation and mean pressure coefficients of all the faces are also studied numerically by CFD for different wind incidence angles. Pressure variation and mean pressure coefficients for all the faces have already been studied experimentally in section 4.2.1. Here, wind effects on the building model is studied from 0° to 180° wind angles at an interval of 30° similar to the wind tunnel test. In order to compare numerically predicted results, pressure contour for the same faces are plotted also here in Fig. 10 as it was plotted in Fig. 9 using wind tunnel results. It can be seen clearly that numerically predicted pressure

contours are converged well with the experimentally predicted results. However, very tiny variation in mean pressure coefficients are observed with respect to the experimental results (Fig. 11(b)).

Maximum positive mean C_p on face (A, I), (B, H), (C, G), (D, F), (J, L), K and E are occurred at 150°, 180°, 180°, 150°, 90°, 0° and 180° respectively. Wind incidence angle is different from experimental one only for face (D, F) considering maximum positive mean C_p . However, almost same value is noticed for 180° also with very tiny variation from 150° on that face. Similar to experimental results, maximum negative mean C_p of all the faces are occurred at same wind incidence angles as in wind tunnel test. Overall study of pressure coefficients depicts a very good agreement of results between experimental and numerical study.

Here also some of the faces undergoes almost zero mean pressure coefficients ($C_p < 0.1$) as in experimentally predicted results. Though these faces have almost zero mean pressure, the magnitude of pressure is largely varied between negative to positive (Fig. 10), so these faces should be designed considering the local pressure coefficients.

4.3 Comparative study

A detail comparison of two different methods considered for the present study has been carried out. More specifically, numerically predicted results are compared

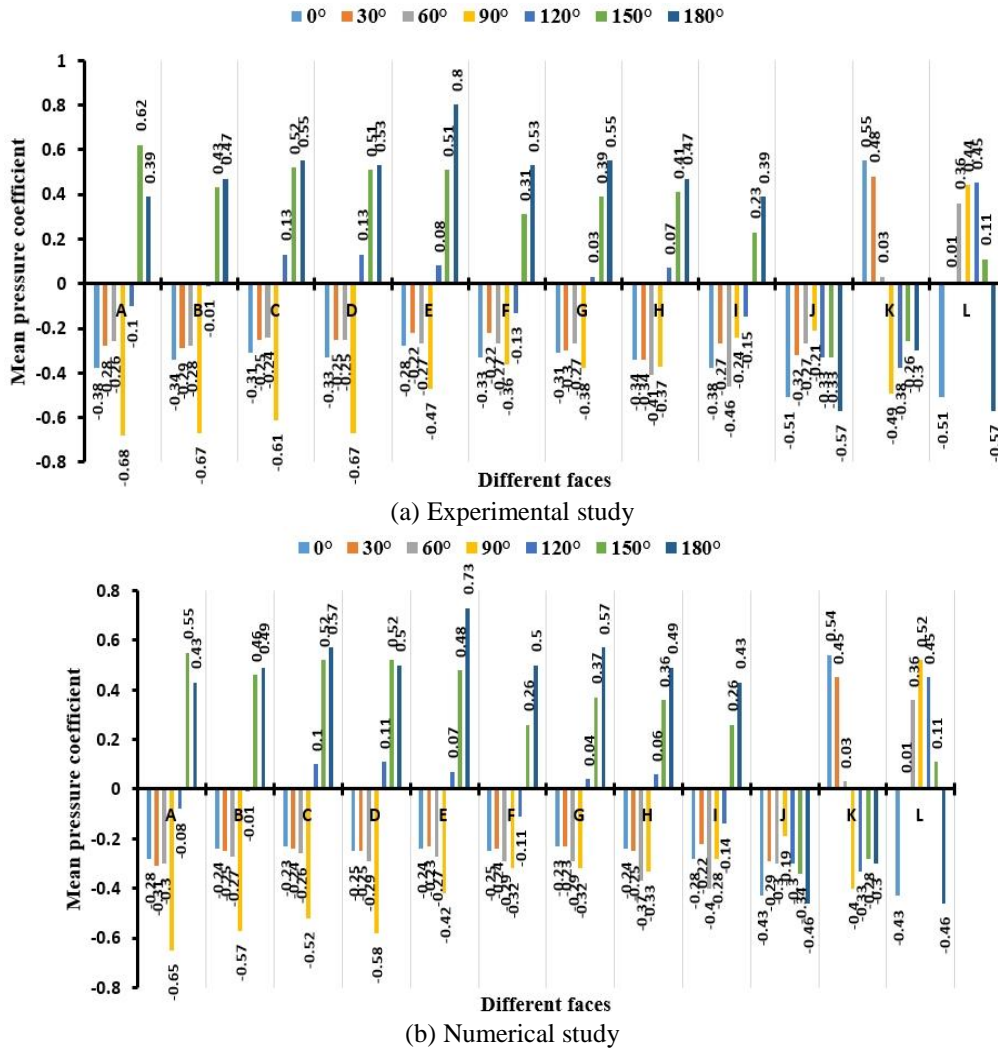


Fig. 11 Mean pressure coefficients for all the faces of the building

with the experimentally predicted results as numerical method offers a good efficiency with respect to wind tunnel test. To investigate more accurately, mean pressure coefficients of different faces are considered.

In order to compare more specifically, mean pressure coefficients of each of the faces and pressure contour are considered. Mean pressure coefficients of all faces for different wind incidence angles are shown in Fig. 11 and pressure contour of some critical faces are plotted in Fig. 9 and 10 by experimental and numerical study respectively. The values found by two methods (experimental and numerical study) are comparable and the magnitudes found by numerical method are within the acceptable limit with respect to wind tunnel results. It is also noticeable that almost zero mean pressure coefficients are absolutely merging the results predicted by two methods. On the other hand, pressure contours (Figs. 9 and 10) predicted from experimental and numerical study are well converged with each other. Very tiny discrepancy is noticed on face F and K between experimentally and numerically predicted pressure contours. These discrepancy has occurred due to mesh pattern throughout the domain. Meshing plays an important

role in case of numerical study as the solution is computed by the finite element operation. The mesh or discretization could be improved through high computational efficient laboratory.

4.4 A detail study for all wind angles

A detail study has been carried out in this section considering all wind incidence angles for all the faces of the building. More specifically, pressure variation on different faces of the building along vertical centerline i.e., along the height of the building is studied for each wind incidence angle. Also, the variation in mean pressure coefficients for each of the face by varying wind incidence angle is studied as a part of detail study. Finally, analytical expressions for each of the face are provided for predicting mean pressure coefficients. This detail study will help the practicing engineers to predict wind pressure coefficients analytically for the building.

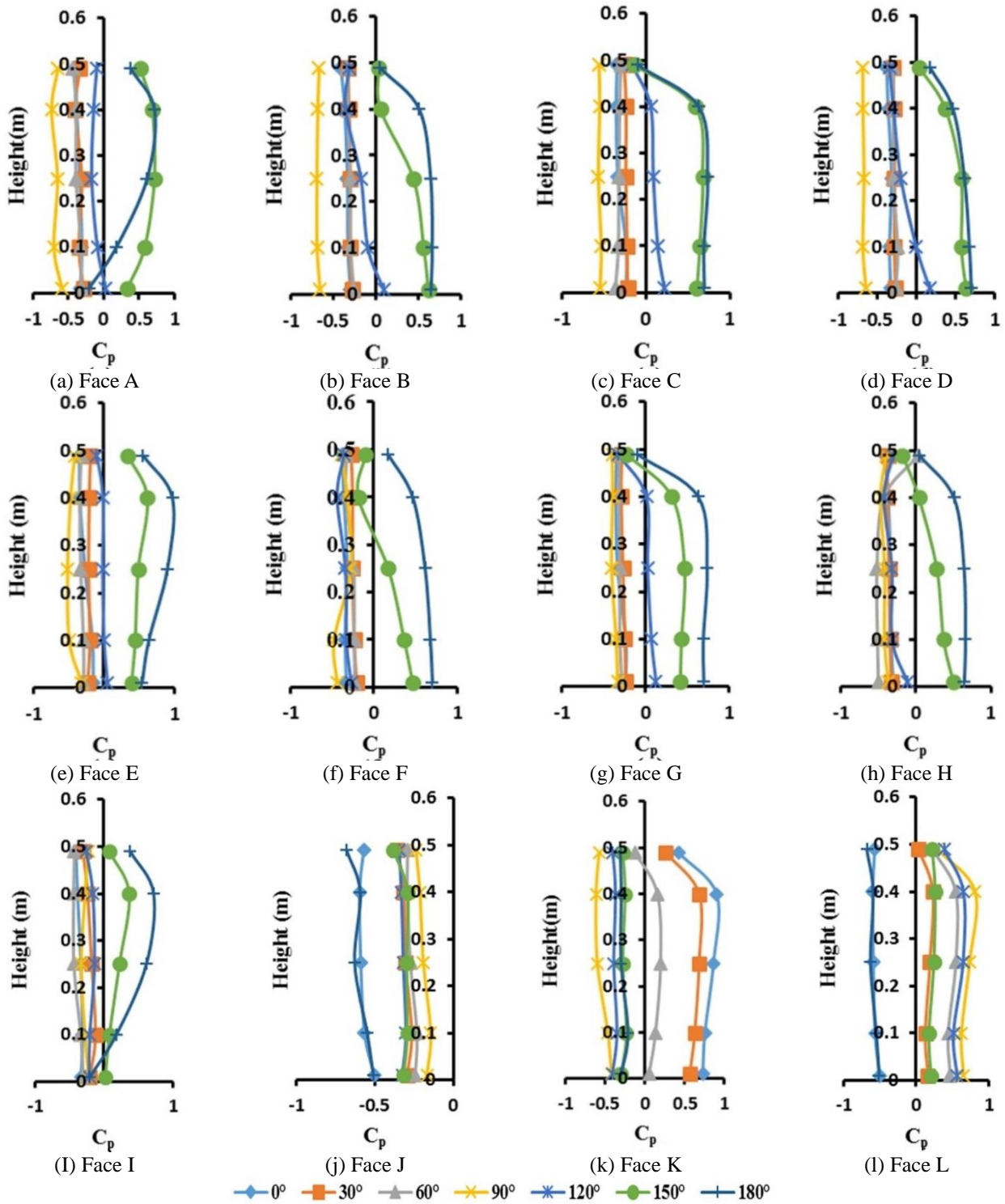


Fig. 12 Pressure variation along vertical centerline for all the faces

First and foremost, variation of pressure coefficients along vertical centerline for different faces of 'E' plan shaped building are plotted in Fig. 12 considering all the wind incidence angles. Vertical pressure variation on face K is varying from parabolic (positive) to almost straight line (negative) with wind angles varies from 0° to 180°. Almost similar pressure variation is noticed on some symmetrical

faces (i.e., face (A, I); (C, G)) about vertical axis for all wind incidence angles. Some abnormal behavior of pressure variation is noticed on face H at 150° wind incidence angle. Positive pressure is noticed at the top portion of this face because of thrust action of wind flow after upwash mechanism. Some positive pressure is observed at the lower portion of face D at 120° wind angle, however most of the

Table 1 Parameters of Fourier polynomials for different faces of the building

Face	ω	Constant parameters				
		a_0	a_1	b_1	a_2	b_2
A	0.02924	-0.09917	0.04675	-0.4656	-0.3292	0.1097
B	0.02687	-0.0985	-0.07233	-0.4287	-0.172	0.2022
C	0.02635	-0.03564	-0.1426	-0.4323	-0.1326	0.2341
D	0.02649	-0.05515	-0.1341	-0.4357	-0.1395	0.252
E	0.02097	0.001822	-0.4231	-0.2564	0.138	0.2612
F	0.02193	-0.06366	-0.2723	-0.2535	0.005675	0.2217
G	0.02373	-0.02881	-0.241	-0.3436	-0.0436	0.1643
H	0.02084	-0.1137	-0.3883	-0.1419	0.1637	0.1285
I	0.000249	-1.27×10^7	1.693×10^7	3.742×10^5	-4.231×10^6	-1.871×10^5
J	9.545×10^{-5}	-1.859×10^8	2.478×10^8	2.453×10^6	-6.195×10^7	-1.076×10^6
K	0.02326	-0.06786	0.426	0.08697	0.1802	0.1697
L	0.02498	-0.1224	-0.47	0.5419	0.06938	0.1276

upper portion is experienced by negative pressure due to interference effects of the limbs close to the face. Pattern of pressure variation along vertical centerline of face K and E is almost equal and opposite in nature from 0° to 180° wind angle as expected due to opposite surfaces with respect to wind angles. Vertical centerline pressure distribution on face J is always negative because no direct wind force is affected on this face. However, almost mirror image pressure variation is noticed on face L along vertical centerline for 0° to 90° and 90° to 180° wind angles.

In the context of detail study on wind pressure coefficients of each of the faces, the variation of mean pressure coefficients with wind incidence angles are required to plot. Also, it is important to quantify mean pressure coefficient for a particular face of the 'E' plan shaped tall building without rigorous calculation. For that reason, it is of utter importance to propose analytical expression for each of the face. To propose analytical expression, the Fourier expansion has been utilized as the sum of *sine* and *cosine* function. The Fourier expansion can be given by

$$f(x) = a_0 + \sum_{i=1}^n \{a_i \cos(i\omega x) + b_i \sin(i\omega x)\} \quad (9)$$

where, a_0 is the constant which is also intercept of the model, ω is the frequency of the signal or, the predictive function. In this equation, i must be truncated at some finite number n to get a proper harmonic polynomial. a_i and b_i are the constants corresponding to the harmonic terms. To propose polynomial for the different faces of the building with the Fourier series as provided in (9), $n=2$ has been chosen for the present problem. So, the Fourier expansion for each of the faces can be given by

$$f(x) = a_0 + a_1 \cos(\omega x) + b_1 \sin(\omega x) + a_2 \cos(2\omega x) + b_2 \sin(2\omega x) \quad (10)$$

where, x is the wind incidence angle in degree and $f(x)$ denotes the mean pressure coefficients for different wind incidence angle for a particular face. All the parameters of the equation for the different faces are provided in Table 1. Also, the curve fitting for different faces of the building using Fourier series expansion are provided in Fig. 13. It

can be seen from the figures that all the predicted curves are fitted well with the test data. To check the accuracy of the fitted models as shown in Table 1 and Fig. 13, three different error measurements have been performed which are sum squared error (SSE) which is also known as residual sum of square (RSS), R^2 value which is widely used statistical measure to check feasibility of the model and root mean square error (RMSE). The expressions for all the three error measurement procedure are given below.

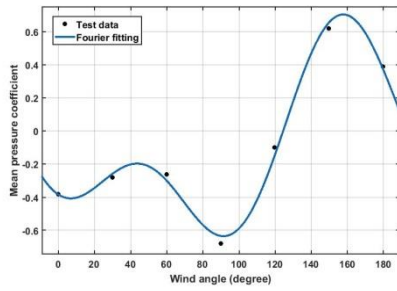
$$SSE = \sum_{i=1}^N \{y_i - f(x_i)\}^2 \quad (11)$$

$$R^2 = 1 - \frac{\sum_{i=1}^N \{y_i - f(x_i)\}^2}{\sum_{i=1}^N (y_i - \bar{y})^2} \quad (12)$$

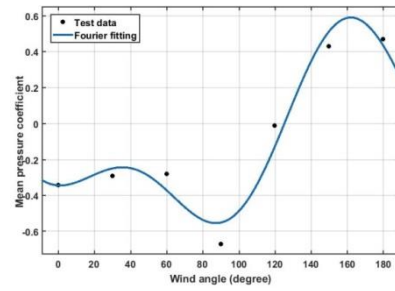
$$RMSE = \sqrt{\frac{1}{N} \sum_{i=1}^N \{y_i - f(x_i)\}^2} \quad (13)$$

where, N is the total number of observation for a model, \bar{y} is the mean of observed data, y_i is the observed value at x_i and $f(x_i)$ is the predicted value at x_i using Fourier series expansion. All the above mentioned errors are plotted in Fig. 14.

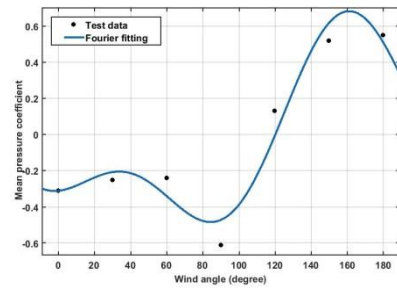
It can be seen from Fig. 14(a) that SSE predicted for all the faces are below 0.1 which is acceptable for the proposed model. Most importantly, most of the values are below 0.03 except face B, C, D which justify the applicability of the proposed expressions. Similarly, all the predicted R^2 values lie between 0.9 and 1 which is very good for fitting any data. Also, the RMSE values are within the permissible limit for all the faces. Thus, the predicted Fourier series expansion for each of the faces can be utilized for predicting mean pressure coefficient on any face for a particular wind incidence angle which may varies from 0° to 180° .



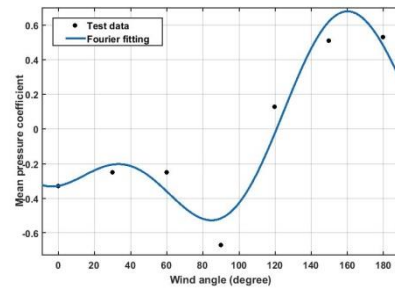
(a) Face A



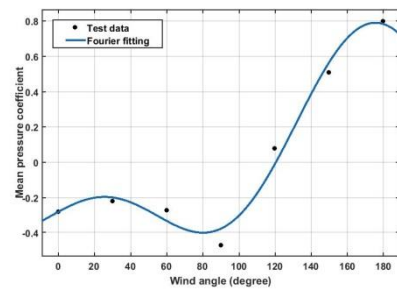
(b) Face B



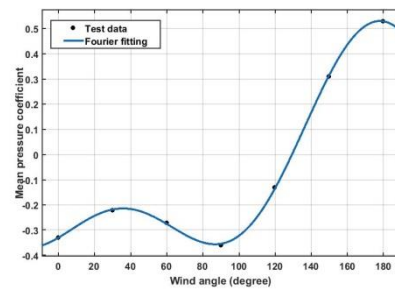
(c) Face C



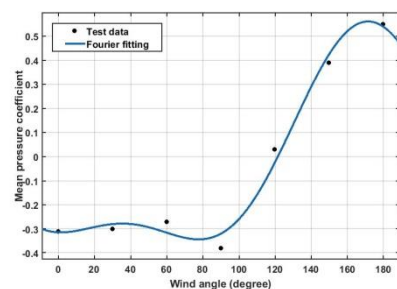
(d) Face D



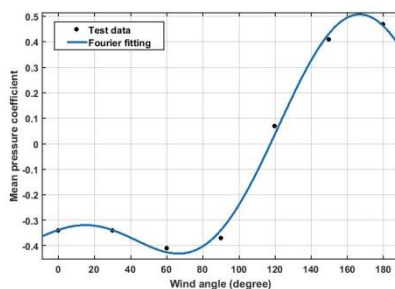
(e) Face E



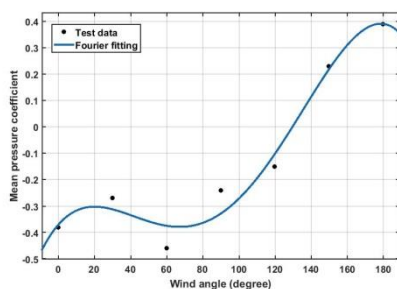
(f) Face F



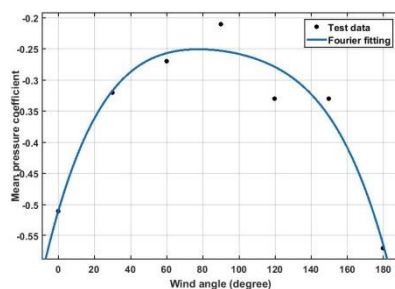
(g) Face G



(h) Face H



(i) Face I



(j) Face J

Continued-

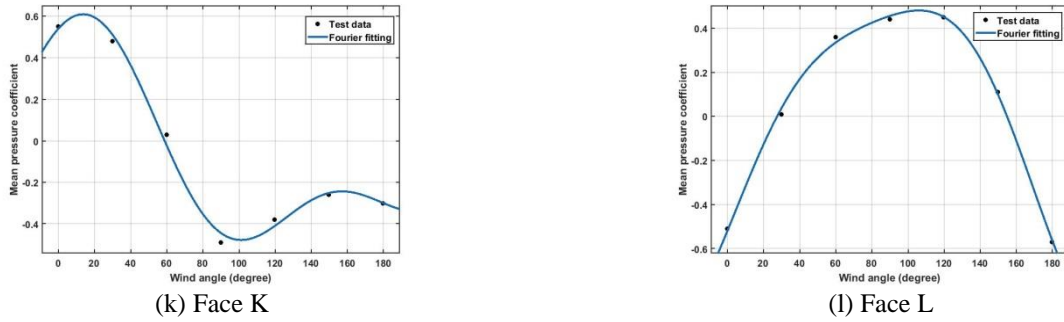


Fig. 13 Curve fitting to predict mean pressure coefficient using Fourier series for different faces

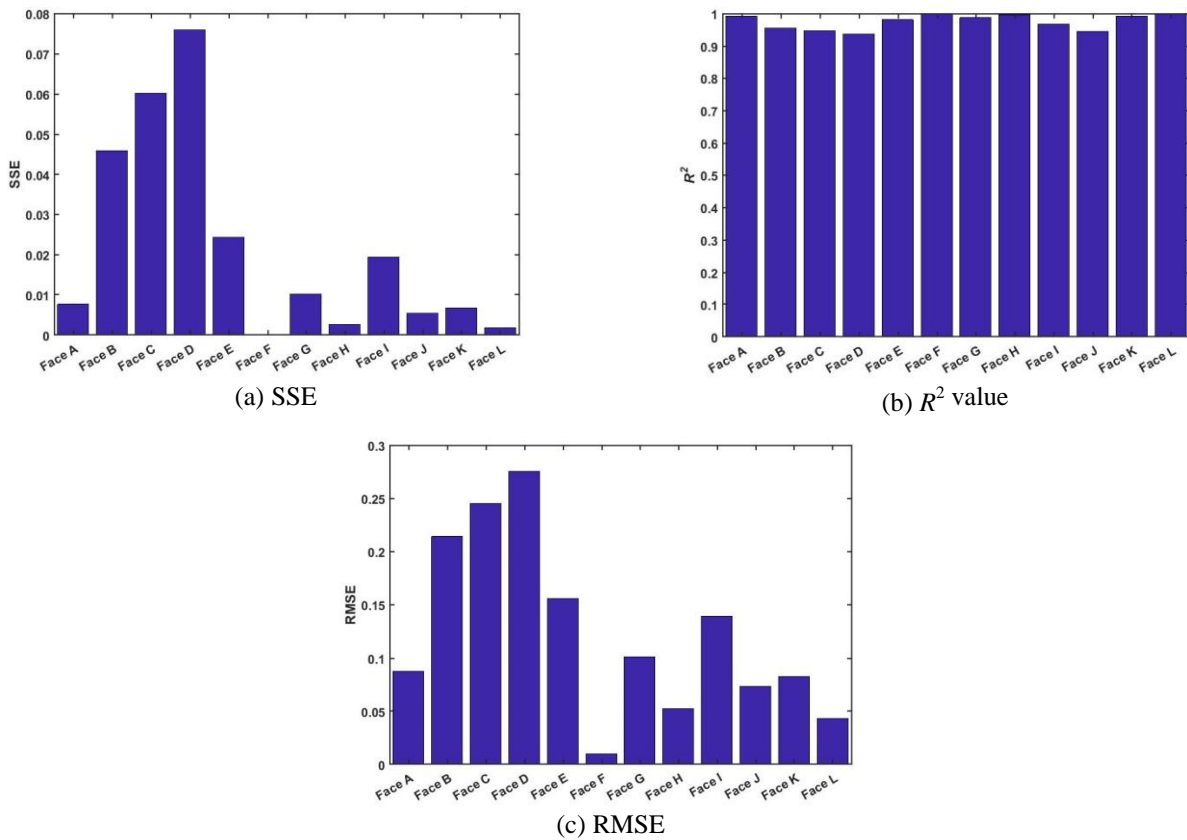


Fig. 14 Different errors of the Fourier series for different faces of the building

5. Conclusions

A comprehensive study has been carried out in this paper to understand wind effects on ‘E’ plan shaped tall building. The study has been conducted with a 1:300 scaled model experimentally as well as numerically using wind tunnel test and CFD technique respectively. Wind tunnel test is already an acceptable method for calculating wind pressure on any type of structure. On the other hand, CFD has emerged a lot in last two decades for predicting wind effects on different types of structure. A clear view of wind flow pattern has been studied using CFD technique which can address the wind flow behavior for different wind incidence angles. Symmetrical wind flow pattern is found

for 0° and 180° wind incidence angle and it was noticed that similar pressure variation has occurred on similar faces for these two wind incidence angles. Highly dynamic behavior of wind flow is noticed at 30° and 120° wind incidence angle. This type of flow pattern is directly affected the building through the pressure variation on the faces located at the wake region.

Mean pressure coefficients are proposed for the different faces of the ‘E’ plan shaped tall building at different wind incidence angles as the main objective of this study. Maximum positive mean C_p is noticed on face E at 180° wind incidence angle and maximum negative mean C_p is occurred on face A at 90° wind angle. However, these two values are not complete for designing the ‘E’ plan shaped

tall building under wind excitation. For the purpose of design, critical mean C_p has been proposed for each of the face. Also, the results found by CFD technique are well-compared with the experimental results which suggests the feasibility of using this technique in predicting wind pressures on building efficiently and accurately. Besides the wind flow pattern and mean pressure coefficients, pressure contours on different faces of the building have also been studied using both the method for all wind incidence angles. A very large variation of pressure (from negative to positive magnitude) is noticed on some faces at skew-wind angle (120°) which results in obtaining almost zero mean C_p on those faces. Further, some analytical expression has been proposed for each of the face of the building using Fourier series expansion. The expressions are predicted for each of the face of the building using *sine* and *cosine* function of wind incidence angle. So, anyone can easily predict mean wind pressure coefficient of a particular face of the building for any wind incidence angle varies from 0° to 180° . The accuracy of the proposed models are measured by three accuracy measurement procedure such as sum square error (SSE), R^2 value and root mean square error (RMSE). It was noticed that all the errors are within the permissible limit. The accuracy may be increased further by computing the wind pressures at an interval lesser than 30° .

References

- Amin, J.A. and Ahuja, A. (2012), "Wind-induced mean interference effects between two closed spaced buildings", *J. Civil Eng. - KSCE*, **16**(1), 119-131.
- AS/NZS 1170-2 (2011), *Australian/New-Zealand Standard, Structural design actions, Part 2: Wind actions*. Sydney, Wellington.
- ASCE 7-10 (2010), *Minimum Design Loads for Buildings and Other Structures*, American Society of Civil Engineering, ASCE Standard, Reston, Virginia.
- Bandi, E.K., Tamura, Y., Yoshida, A., Chul Kim, Y. and Yang, Q. (2013), "Experimental investigation on aerodynamic characteristics of various triangular-section high-rise buildings", *J. Wind Eng. Ind. Aerod.*, **122**, 60-68.
- Bashor, R., Bobby, S., Kijewski-Correa, T. and Kareem, A. (2012), "Full-scale performance evaluation of tall buildings under wind", *J. Wind Eng. Ind. Aerod.*, **104-106**, 88-97.
- BS 6399-2 (1997), *Loading for buildings- Part 2: Code of practice for wind loads*, British Standard, London, UK.
- Chakraborty, S., Dalui, S.K. and Ahuja, A.K. (2014), "Wind load on irregular plan shaped tall building-a case study", *Wind Struct.*, **19**(1), 59-73.
- Cheng, Y., Lien, F.S., Yee, E. and Sinclair, R. (2003), "A comparison of large eddy simulations with a standard k- ϵ Reynolds-averaged Navier-Stokes model for the prediction of a fully developed turbulent flow over a matrix of cubes", *J. Wind Eng. Ind. Aerod.*, **91**(11), 1301-1328.
- Cheung, J.O.P. and Liu, C.H. (2011), "CFD simulations of natural ventilation behaviour in high-rise buildings in regular and staggered arrangements at various spacings", *Energ. Buildings*, **43**(5), 1149-1158.
- Dalui, S.K. (2008), "Wind effects on tall buildings with peculiar shapes." Indian Institute of Technology Roorkee, India.
- Endo, M., Bienkiewicz, B. and Ham, H.J. (2006), "Wind-tunnel investigation of point pressure on TTU test building", *J. Wind Eng. Ind. Aerod.*, **94**(7), 553-578.
- Franke, J., Hirsch, C., Jensen, A.G., Krüs, H.W., Schatzmann, M., Westbury, P.S., Miles, S.D., Wisse, J.A. and Wright, N.G. (2004), "Recommendations on the use of CFD in wind engineering", *International Conference on Urban Wind Engineering and Building Aerodynamics: COST C14: Impact of Wind and Storm on City life and Built Environment*.
- Gomes, M.G., Moret Rodrigues, A. and Mendes, P. (2005), "Experimental and numerical study of wind pressures on irregular-plan shapes", *J. Wind Eng. Ind. Aerod.*, **93**(10), 741-756.
- Gomes, M.G., Rodrigues, A.M. and Mendes, P. (2003), "Wind effects on and around L- and U-shaped buildings", *Proceedings of the 5th International Conference on Urban Climate (ICUC5)*, Lodz, Poland.
- Gu, M. and Quan, Y. (2004), "Across-wind loads of typical tall buildings", *J. Wind Eng. Ind. Aerod.*, **92**(13), 1147-1165.
- Hargreaves, D.M. and Wright, N.G. (2007), "On the use of the k- ϵ model in commercial CFD software to model the neutral atmospheric boundary layer", *J. Wind Eng. Ind. Aerod.*, **95**(5), 355-369.
- Huang, M.F., Lau, I.W.H., Chan, C.M., Kwok, K.C.S. and Li, G. (2011), "A hybrid RANS and kinematic simulation of wind load effects on full-scale tall buildings", *J. Wind Eng. Ind. Aerod.*, **99**(11), 1126-1138.
- Huang, S., Li, Q.S. and Xu, S. (2007), "Numerical evaluation of wind effects on a tall steel building by CFD", *J. Constr. Steel Res.*, **63**(5), 612-627.
- IS 875 (Part 3) (2015), *Indian standard code of practice for design wind load on building and structures*, New Delhi, India.
- Kim, Y.C. and Kanda, J. (2013), "Wind pressures on tapered and set-back tall buildings", *J. Fluid. Struct.*, **39**, 306-321.
- Kim, Y.M. and You, K.P. (2002), "Dynamic responses of a tapered tall building to wind loads", *J. Wind Eng. Ind. Aerod.*, **90**(12-15), 1771-1782.
- Kim, Y.M., You, K.P. and Ko, N.H. (2008), "Across-wind responses of an aeroelastic tapered tall building", *J. Wind Eng. Ind. Aerod.*, **96**(8-9), 1307-1319.
- Li, B., Liu, J. and Li, M. (2013), "Wind tunnel study on the morphological parameterization of building non-uniformity", *J. Wind Eng. Ind. Aerod.*, **121**, 60-69.
- Li, Q.S., Fang, J.Q., Jeary, A.P. and Wong, C.K. (1998), "Full scale measurements of wind effects on tall buildings", *J. Wind Eng. Ind. Aerod.*, **74-76**, 741-750.
- Li, Q.S., Fu, J.Y., Xiao, Y.Q., Li, Z.N., Ni, Z.H., Xie, Z.N. and Gu, M. (2006), "Wind tunnel and full-scale study of wind effects on China's tallest building", *Eng. Struct.*, **28**(12), 1745-1758.
- Li, Q.S., Xiao, Y.Q., Fu, J.Y. and Li, Z.N. (2007), "Full-scale measurements of wind effects on the Jin Mao building", *J. Wind Eng. Ind. Aerod.*, **95**(6), 445-466.
- Li, Y. and Li, Q. (2016), "Across-wind dynamic loads on L-shaped tall buildings", *Wind Struct.*, **23**(5), 385-403.
- Mukherjee, S., Chakraborty, S., Dalui, S.K. and Ahuja, A.K. (2014), "Wind induced pressure on 'Y' plan shape tall building", *Wind Struct.*, **19**(5), 523-540.
- Swaddiwudhipong, S. and Khan, M.S. (2002), "Dynamic Response of Wind-Excited Building Using CFD", *J. Sound Vib.*, **253**(4), 735-754.
- Tanaka, H., Tamura, Y., Ohtake, K., Nakai, M. and Kim, Y.C. (2012), "Experimental investigation of aerodynamic forces and wind pressures acting on tall buildings with various unconventional configurations", *J. Wind Eng. Ind. Aerod.*, **107-108**, 179-191.
- Wang, F., Tamura, Y. and Yoshida, A. (2013), "Wind loads on clad scaffolding with different geometries and building opening ratios", *J. Wind Eng. Ind. Aerod.*, **120**, 37-50.
- Yi, J. and Li, Q.S. (2015), "Wind tunnel and full-scale study of wind effects on a super-tall building", *J. Fluid. Struct.*, **58**, 236-

253.

Zhang, A., Gao, C. and Zhang, L. (2005), "Numerical simulation of the wind field around different building arrangements", *J. Wind Eng. Ind. Aerod.*, **93**(12), 891-904.

AD